

Regional climate model projections for North-East Italy

G. Massaro¹ and P. Lionello²

¹ ARPA Veneto, Servizio Centro Meteorologico, Teolo (PD), Italy

² Università del Salento, Dipartimento di Scienze e Tecnologie Biologiche ed Ambientali, Lecce (LE), Italy

Correspondence to: G. Massaro (giovanni.massaro@arpa.veneto.it)

Abstract

This study has analyzed an ensemble of EURO-CORDEX high resolution (0.11 degs) regional climate model (RCM) simulations of the low emission RCP2.6 and high emission RCP8.5 scenarios for North-Eastern Italy for the 21st century covering. It has considered the seasonal anomalies of temperature, precipitation and annual anomalies of heat-wave duration (HWDI) and intense precipitation totals (R95pTOT). Three 30-year periods have been selected: a baseline period (from 1976 to 2005), near future (2021-2050) and far future (2071-2100). Results show the large differences between a low and a high emission scenario for climate change in North-East Italy. In the former case temperature and precipitation changes tends to stop in the second part of the 21st century. In the latter climate change continues along the whole century and substantial warming (+5°C in summer, +4°C in winter), increase of winter precipitation (+15%) and decrease of summer precipitation (-10%) are expected in the far future. Warming is larger in the mountain and Alpine region than in coastal and flat areas. Further, particularly in the mountain areas there is an increase of duration of heat waves (reaching 45 days in the 2071-2100) and of intense precipitations (up to +140%).

Keywords: climate projections, regional climate models, temperature, precipitation, extremes, North-East Italy

1 Introduction

The Earth's climate at scales from global to regional is currently changing and it is expected to profoundly change in the next future, because of increasing anthropogenic greenhouse gas emissions, land use and aerosol concentration changes (IPCC, 2013).

Changes in future climate are generally investigated by Global Climate Models (GCM), which simulate climate evolution at a spatial resolution of about 100 km under assumption of different emission scenarios. The resolution of the GCMs does not allow to describe processes occurring at regional and sub-regional scale that are strongly affected by orographic features and land-sea distribution. Regional climate models (RCM) can achieve a resolution one order of magnitude larger than GCMs. The adopted procedure is called dynamical downscaling. It consists in the one-way nesting of a RCM in the grid of a driving GCM, which provides the boundary and initial conditions for the regional simulations (Giorgi and Mears, 1999). An alternative approach is statistical downscaling (Wilby et al., 1998), which is based on empirical relations connecting large scale drivers to regional climate conditions.

The evaluation of the climate change at regional scale is essential in order to investigate climate change impacts at a spatial scale that is relevant for human activity and ecosystems. Starting from the hazard assessment – such as temperature enhancement and change in the precipitation regime – and accounting for exposure and vulnerability of the impacted sectors or systems, future risks can be evaluated. An accurate computation of future climate scenarios and the inherent uncertainty is required for developing adaptation strategies and assessing the importance of mitigation actions (IPCC, 2014).

The relation between climate change in the Mediterranean region and global warming has been well established (Lionello and Scarascia, 2018). A larger warming has been found in some areas of this basin with respect to the global one, as well as differences in the warming between north and south land areas. Warming is expected to be particularly large for the land areas located north of the basin, locally up to 100% larger than global warming (Lionello and Scarascia, 2018). Pronounced decrease in precipitation, especially in the warm season, is expected with exception for the northern Mediterranean areas (e.g. the Alps) in winter, where the trend is opposite (Gao et al., 2006; Giorgi and Lionello, 2008; Coppola and Giorgi, 2010). Global warming will further increase the existing

difference in intensity of precipitation and hydrological extremes between north and south Mediterranean areas (Lionello and Scarascia, 2020).

The Mediterranean region is characterized by complex morphology and land-sea distribution (Lionello et al. 2012). Climate change in the Mediterranean area is expected to be stronger with respect to the global one (Giorgi, 2006; Giorgi and Lionello, 2008). It represents a situation where advantages of RCMs are particularly important (Planton et al., 2012). Many orographically-induced fine scale structures in the precipitation change signal are reproduced only by the regional climate models at high spatial resolution, unlike the global models (Giorgi and Lionello, 2008; Torma et al., 2015).

Zampieri et al. (2010) assessed the climate change signal in the Northern Adriatic by using regional models (PRUDENCE and ENSEMBLE projects) at a resolution from 25 to 50 km. A significant warming for the period 2071-2100 with respect to the 1961-1990 is expected, up to 4°C in winter and 5.5°C in summer. The precipitation is expected to increase (from +20 to +40%) in most land regions of the considered domain in winter. On the other hand, the precipitation is expected to decrease in summer over most of the domain, around -10% in the Northern boundary. However, many characteristics of the geographical precipitation trends are not statistically significant and hence they are not yet fully established. In summer, over the central Alpine mountains, the large-scale reduction in precipitation found in the driving GCMs is weakened by using regional models at 0.44° resolution, and turns even positive in RCMs at the enhanced 0.11° resolution (Torma et al., 2015).

In this study the state-of-the-art regional models within the project EURO-CORDEX¹ (Jacob et al., 2014) will be considered in order to study the possible climate scenarios, in terms of temperature and precipitation, in the area of North-East Italy with the enhanced spatial resolution of 0.11° (about 12.5 km). In particular, the anomaly of the temperature and precipitation is computed for the ‘near future’ (2021-2050) and ‘far future’ (2071-2100) with respect to a reference period (1976-2005). The anomaly of some extreme events – heat wave duration index (HWDI) and 95th percentile of daily precipitation distribution (R95pTOT) – is also investigated.

Section 2 describes the model dataset used in this study. In Section 3 is explained how the data analysis is conducted. The results are presented in Section 4. Conclusions are given in Section 5.

¹EURO-CORDEX Coordinated Downscaling Experiment - European Domain <http://www.euro-cordex.net/>

2 Dataset

2.1 Regional climate models

CORDEX experiments consist of RCM simulations - obtained by dynamical downscaling from GCMs - representing different future socio-economic scenarios. There are different combinations of RCMs and GCMs, providing the latter the boundary conditions in all the experiments. The considered GCMs comes from the CMIP5 (5th phase of the Coupled Model Intercomparison Project) archive (Taylor et. al, 2012). The climate model outputs have *historical* runs, which typically covers a period from 1950 to 2005 and can be used as a reference period for comparison with scenario runs for the future. On the other hand *scenario* runs, typically from 2006 to 2100, are climate projection experiments using different *Representative Concentration Pathways* (RCP) forcing scenarios (Moss et al., 2010). Each RCP corresponds to a different radiative forcing onto the global climate due to the contribution of greenhouse gas emission. RCP2.6 corresponds to a radiative forcing of 2.6 W/m^2 (2°C of warming at 2100 with respect to the pre-industrial period (Meinshausen et al., 2006)), RCP4.5 to 4.5 W/m^2 (intermediate scenario) and RCP8.5 to 8.5 W/m^2 (the so-called *business as usual*, from 3°C to 5.5°C of warming (IPCC, 2013)). RCMs from EURO-CORDEX have a spatial resolution of 0.11° that corresponds to about 12.5 km in the domain of Europe area (EUR-11, Jacob et al., 2014). They yields several daily mean meteorological variables, dealing among all with pressure, temperature, humidity, wind, precipitation.

Climate projections have several intrinsic uncertainties (Giorgi, 2005): the radiative forcing due to the future greenhouse gas emissions (eg.: RCP2.6, 4.5, 8.5, ...); the representation of physical processes that are not sufficiently well understood or resolved (e.g.: cloud physics, surface energetic balance, ...); the natural variability of the climate system at multiple spatial and time scales, which could possibly hide the anthropic contribution to the climate change (Cubash et al, 2001).

2.2 Dataset description

The dataset has been obtained from the [Earth System Grid Federation](https://esgf-data.dkrz.de/projects/esgf-dkrz/) (ESGF)², an international collaboration that provide several climate model outputs, including CORDEX models. The output is distributed into NetCDF format, self-describing binary file containing all relevant information about data (metadata). The data within are divided in two parts: a header containing the metadata and the body where the actual data are shared. They are gridded dataset with time evolution at a daily

²<https://esgf-data.dkrz.de/projects/esgf-dkrz/>

temporal resolution. NetCDF files can be read by most data analysis software. In this work CDO (Climate Data Operator) is used to compute climate statistics (Schulzweida, 2019).

3 Methodology

3.1 Selection of models

Within the EURO-CORDEX there are many experiments, as produced from combinations of GCMs and RCMs. For each pair there is also several ensemble runs from different initial conditions or physical parametrization. In this work only the control runs is considered, namely that with the not-perturbed initial conditions; the models with both the more conservative scenario (RCP2.6) and the more extreme (RCP8.5) are considered. Since in this study the daily temperature and precipitation are the variables of interest, only the models with the variables *near-surface air temperature, daily minimum near-surface temperature, daily maximum near-surface temperature and precipitation* are considered. Accounting for the requirements above and searching for the most larger number of models, a total of 14 models are considered for RCP8.5 and 8 models for RCP2.6 (Table 1). For the RCP8.5 there is actually a total of 15 experiments, but one of these (the GCM/RCM IPSL-CM5A-MR/INERIS-WRF331F) is discarded because considered as outliers in the precipitation values over the Adriatic Sea. In a successive study this aspect will be better examine.

GCM	RCM	Resolution	RCP2.6	RCP4.5	RCP8.5
CNRM-CM5	CCLM4-8-17	0.11°	-	X	X
CNRM-CM5	RCA4	0.11°	-	X	X
EC-EARTH	CCLM4-8-17	0.11°	X	X	X
EC-EARTH	HIRHAM5	0.11°	X	X	X
EC-EARTH	RACMO22E	0.11°	X	X	X
EC-EARTH	RCA4	0.11°	X	X	X
HadGEM2-ES7	CCLM4-8-17	0.11°	-	X	X
HadGEM2-ES	RACMO22E	0.11°	X	X	X
HadGEM2-ES	RCA4	0.11°	X	X	X
IPSL-CM5A-MR	RCA4	0.11°	-	X	X
MPI-ESM-LR	CCLM4-8-17	0.11°	-	X	X
MPI-ESM-LR	RCA4	0.11°	X	X	X
MPI-ESM-LR	REMO2009	0.11°	X	X	X
NCC-NorESM1-M	HIRHAM5	0.11°	-	X	X

Table 1. Regional climate simulations extracted from EURO-CORDEX project that are considered in this study. GCM stands for Global Climate Model, RCM for Regional Climate Model, RCP refers to different Representative Concentration Pathway, the X marks available simulations.

3.2 Data analysis

The output of experiments from ESGF is available on the entire Europe domain on rotated latitude/longitude grids differing among models. Here, individual model data are interpolated by a distance-weighted average remapping on a common grid with a lat-lon resolution of 0.10° (about 11 km), which covers the area of Triveneto (Veneto, Trentino-Alto Adige and Friuli-Venezia Giulia) from 10.10° to 14.20° in longitude and from 44.55° to 47.35° , in latitude.

Anomalies of temperature (precipitation) for RCP2.6 and RCP8.5 projections are computed with respect to the 30-year mean value of the reference time period 1976-2005 for mean winter (December, January, February, DJF) and summer (June, July, August, JJA) seasonal values. The choice of this reference period represents a compromise among the last CMIP5 20-year reference period (1986-2005) of historical simulations and the time period of the observational dataset that will be used for model validation in the continuation of this study. The additional 10 years are meant to allow robust statistics accounting for inter-annual and inter-decadal variability in the observations. The anomaly is calculated as a difference for the temperature and as a percentage change for precipitation with respect to the reference period. Values are averages for the Triveneto area. The ensemble mean of all models is used as 'best future projection' and the spread among them as its uncertainty (see Giorgi, 2015 for a review). In order to estimate the uncertainty in the different radiative forcing scenarios, the low emission scenario (RCP2.6) and the high emission (RCP 8.5) are compared.

The uncertainty of the model ensemble is also investigated. In order to depict the inter-model uncertainty, the timeseries of the annual anomaly temperature (precipitation) up to 2100 with respect to the reference period 1976-2005 are plotted for all the members of the RCP8.5 ensemble. For estimate the inter-model uncertainty, the anomalies of temperature (and precipitation) for two future periods - 2021-2050 and 2071-2100 with respect to the reference period - are calculated in the RCM ensemble (for each season and RCP). For the temperature, the anomalies are simple differences between future and reference periods averaged in the considered domain. Regarding the precipitation, the anomaly is given in terms of percentage change between the two periods. All the anomalies are plotted in boxplots, with upper and lower limits at 25th and 75th percentile and whiskers at 10th and 90th percentile.

In order to estimate the trend, the Sehn'slope of the anomalies of the ensemble is considered (for each season, RCP and future periods). Boxplots are used to assess the agreement among the models.

In particular, in order to have a positive or negative trend the 90th percentile of the ensemble is required to have the same sign.

In order to assess the geographic distribution of the temperature (precipitation) anomalies, the ensemble mean temperature (precipitation) anomaly for the RCP2.6 and RCP8.5, winter and summer is calculated in each grid point for two the near and far future with respect to the reference period. For testing the agreement among the models, the multi-model mean at each grid point should be larger compared to inter-model variability, calculated as standard deviation among different models with respect to the ensemble mean in each grid point (Stocker et al., 2013).

3.3 Climate indices

In order to assess hazards and suggest potential impacts on society and natural ecosystems, some climate indices related to extreme events can be computed.

Temperature extreme events can entail many impacts relating to (among all) thermal comfort, primary sector, energy sector. A common used index is the heat wave duration index (HWDI); here, it is calculated by considering 5 consecutive days in which the maximum temperature is 5°C larger than the average of the reference period for that day of the year (Giorgi et al., 2014; Gallina and Giorgi, 2008). This index is calculated only for the summer and the reference temperature mean is calculated for each day by a 5-days moving average.

Extreme rainfall events in terms of intensity may also have serious impacts, such as flooding events or erosion phenomena. A signal for detecting these events is the cumulative rainfall beyond the 95th percentile of the daily precipitation distribution (R95pTOT, Giorgi et al., 2014); this index identifies the precipitation intensity threshold where there is the 5% of the most intense events.

For both these indices the anomaly in each grid point for the two future periods with respect to the reference period are computed by considering the ensemble mean; for testing the agreement among the models, the same method used for temperature and precipitation anomaly map is used.

4 Results

4.1 Temperature

The timeseries of the annual anomaly of temperature until 2100 with respect to the reference time period 1976-2005 for RCP2.6, RCP4.5 and RCP8.5 ensemble means and selected seasons (winter or summer) is shown in Figure 1. By considering the most conservative scenario RCP2.6 and most extreme scenario RCP8.5, the temperature anomaly is between 1.5°C and 4.5°C at 2100 in winter, and between 1.5 and 5.5°C at 2100 in summer.

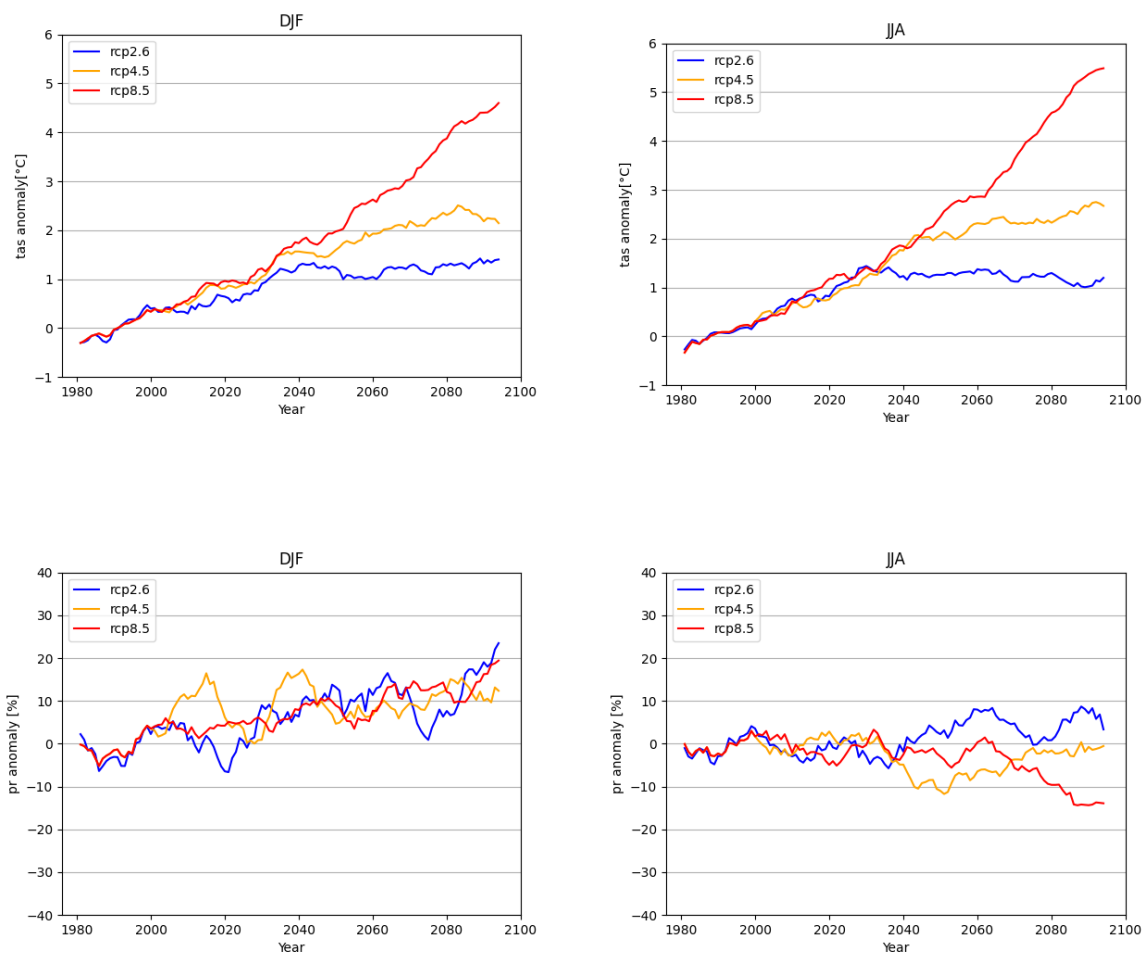


Figure 1. (Upper panel) Annual temperature anomaly with respect to the reference period 1976-2005 for the three RCP scenarios in winter (left) and summer (right). Values are averaged over all the considered spatial domain and represent the ensemble mean and cover the period from 1976 to 2100. A 11-year moving average has been applied to each timeseries. RCP refers to Representative Concentration Pathways. (Lower panel) Same as the upper panel, except it shows the annual precipitation anomaly (as percentage difference).

In addition to the uncertainty due to the different RCPs, there is the uncertainty related to the different models, which are characterized by different physics and parametrization. The anomaly of temperature for all the models with RCP8.5 is displayed in Figure 2. The temperature uncertainty is within 2.5°C at 2100 for winter and it increases to 4°C in summer.

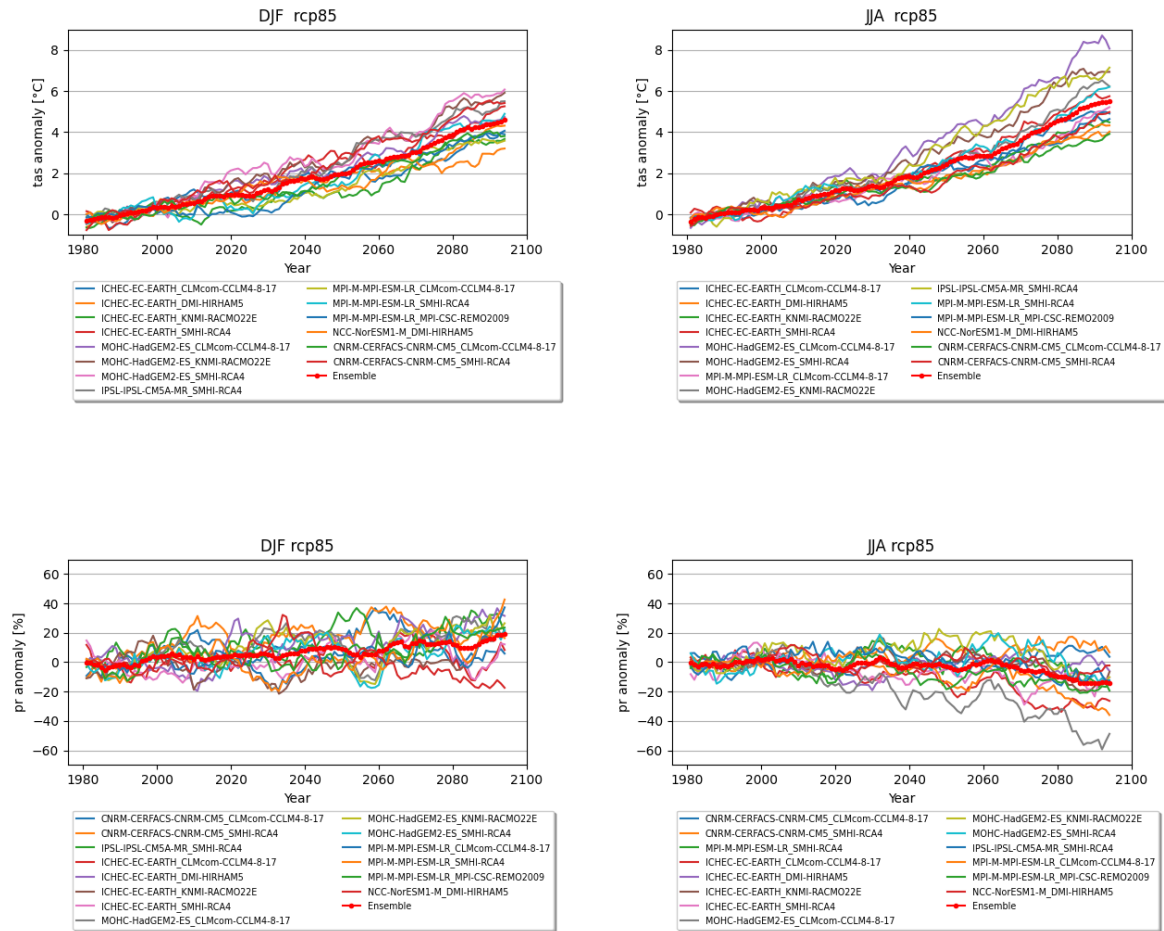


Figure 2. Same as Figure 1 but with the individuals ensemble members of RCP8.5. Ensemble mean is shown with thick red line. The name of the model is in the form GCM_RCM, being GCM global climate model and RCM regional climate model. A moving average with a window size of 11 years has been applied to each curve.

The anomaly for the two future periods, 2021-2050 and 2071-2100, for the model ensemble for the different forcing scenarios and summer and winter is displayed by boxplots in Figure 3. By considering 25th/75th percentile (box), for RCP2.6 the anomaly is between 1°C and 1.5°C both in the near and far future and winter and summer. For RCP8.5 the anomaly is within 1 and 2°C in the near future; in the far future it is between 3.5°C and 5°C and from 4°C to 5.5°C in winter and summer, respectively. Therefore, the temperature anomaly is larger in summer.

The significance of the trends is investigated by the boxplots considering 10th/90th percentile (whishers) in Figure 4. The temperature has a significant positive trend in all seasons and periods, with exception of the RCP2.6 in the summer. By considering the ensemble mean in the far future, there is an increase between 2°C/100y (RCP2.6) and 6°C/100y (RCP8.5) in winter, and around 6.5°C/100y (RCP8.5) in summer.

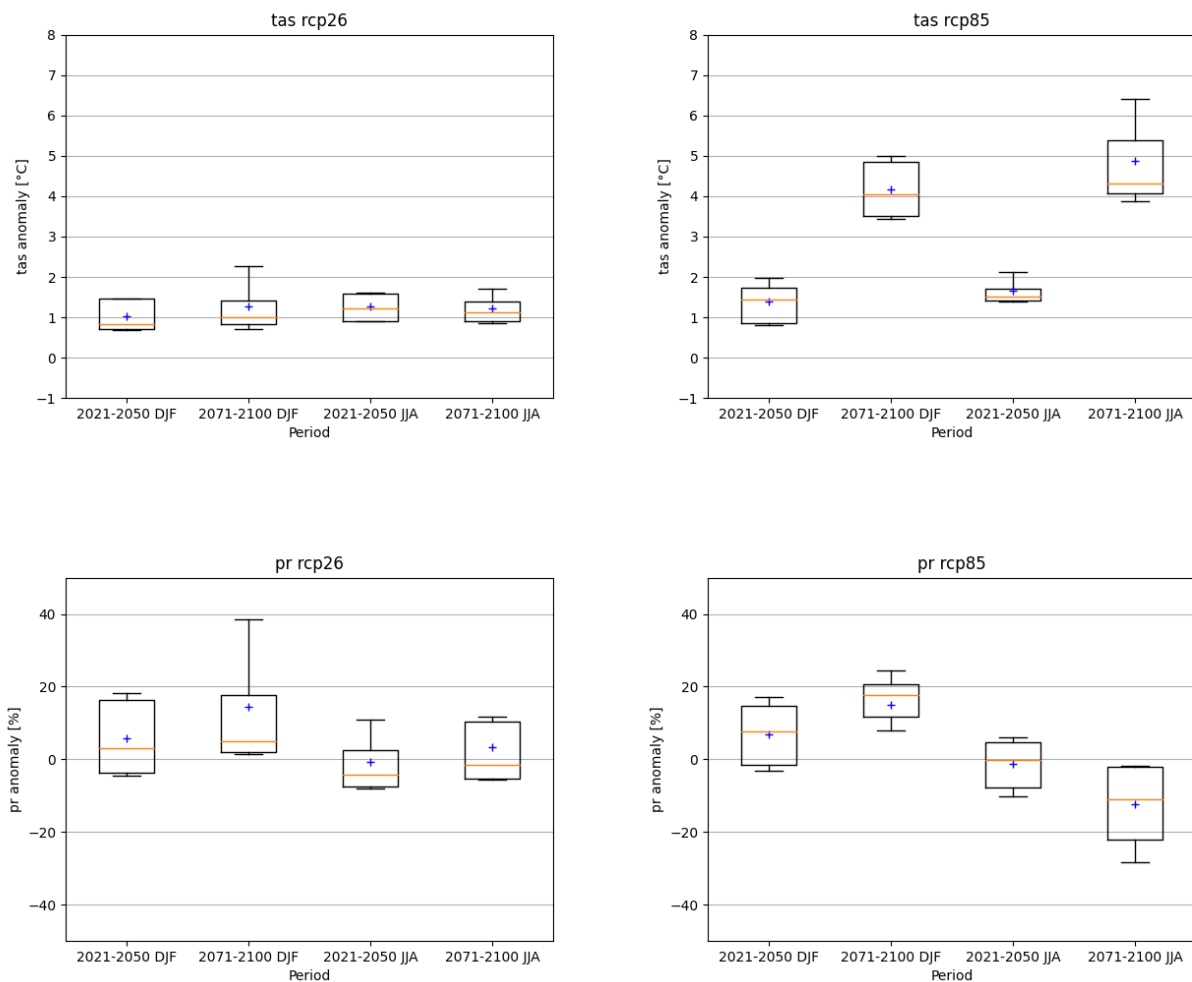


Figure 3. (Upper panel) Anomalies of the winter (DJF) and summer (JJA) temperature for the periods 2021-2050 and 2071-2100 with respect to the reference period 1976-2005 in the RCM ensemble. Left panel refers to RCP2.6 and right panel to RCP8.5. Upper and lower limits of the box indicate the 25th and 75th percentile, the whiskers correspond to 10th and 90th percentile, respectively, the red horizontal line is the median value. The blue cross indicates the anomaly of the ensemble mean. (Lower panel) Same as upper panel, except it shows anomalies of precipitation.

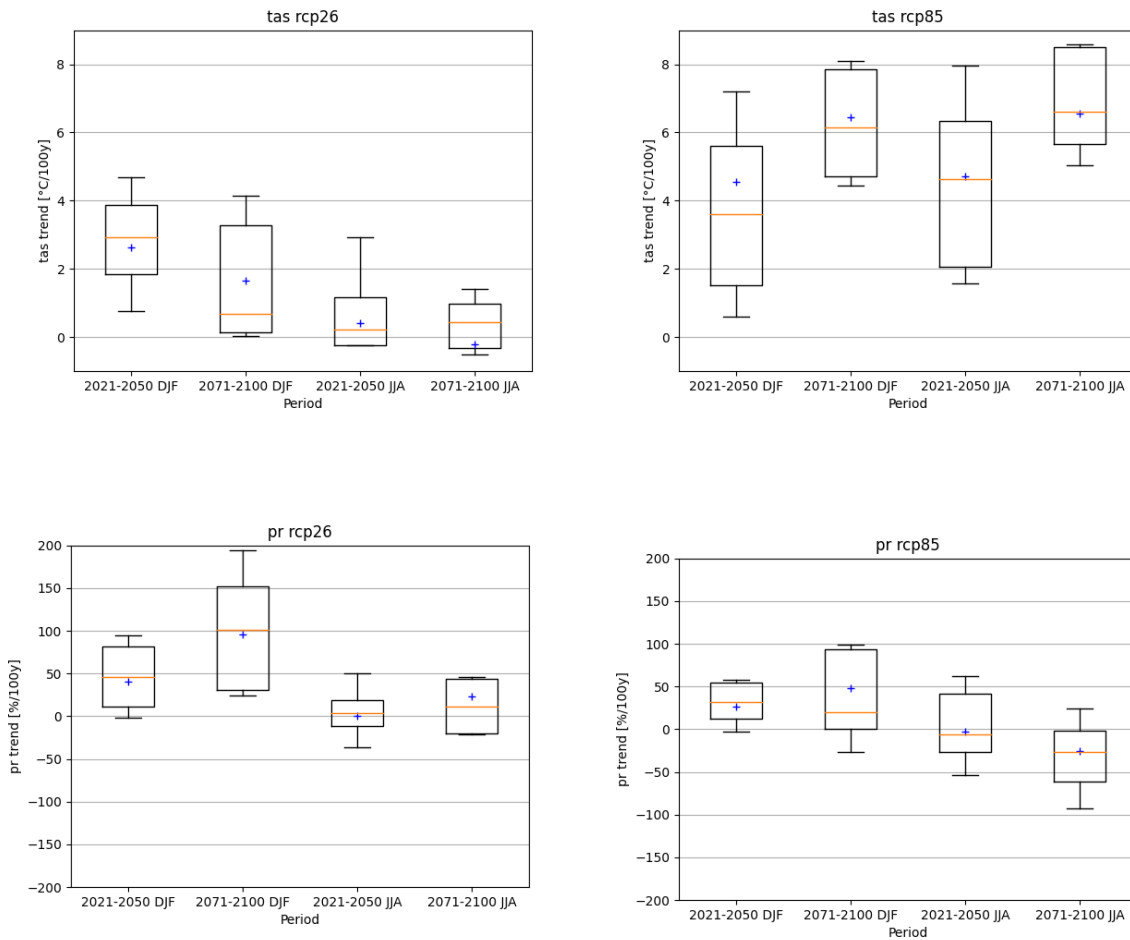


Figure 4. Same as Figure 3, except it shows trends (units: °C/100y or %/100y).

The geographical distribution of the ensemble mean temperature anomaly for RCP2.6 and RCP8.5, near future and far future with respect to the reference period is displayed in Figure 5 for winter and summer. Crosses indicate the grid points where the models agreement is low, i.e. ensemble mean anomaly is lower than inter-model standard deviation. For all temperature anomaly scenarios there is statistical significance throughout the land areas. The area less affected by the warming are coastal and flat lands, whereas the mountain areas are the more affected by the warming, especially in the winter season. In winter, in 2021-2050 the temperature anomaly is within 0.5°C and 1°C in flat lands and from 1°C to 1.5°C in mountain areas for RCP2.6; the temperature anomaly increases from 1°C to 1.5°C in flat lands and from 1.5°C to 2°C in the pre-Alps and Alps areas for RCP8.5. In the far future, the warming is within 1°C and 1.5°C with peaks from 1.5°C to 2°C in the pre-Alps for RCP2.6, and it increases from 3.5°C to 4°C in coastal or flat lands, and it further increases from 5°C and 5.5°C in the Alps areas for RCP8.5. The latter could be related to the melting of snow and

glaciers and subsequent reduction in the surface albedo. For the summer season, the warming is geographically more uniform with respect to the winter, it is between 1°C and 1.5°C for RCP2.6 in both 2021-2050 and 2071-2100; for RCP8.5 the warming is between 1.5°C and 2°C for 2021-2050 and it increases from 4.5° to 5°C in flat lands and from 5°C to 6°C in mountain areas in the far future.

4.2 Precipitation

For the precipitation the same quantities of the temperature are computed, with the exception that for precipitation the anomaly is calculated as a percentage change with respect to the reference period.

Figure 1 shows the anomaly of the ensemble mean for the RCPs until 2100 with respect to the reference period for winter and summer. By considering the most discordant RCPs, the precipitation anomaly reaches from +15 to +25% at 2100 in winter; if the summer is considered, the scenarios do not agree and the anomaly reaches +5% with RCP2.6 and -15% with RCP8.5.

In Figure 2 there is the spread among the several models for RCP8.5 for winter and summer. The uncertainty is between +40% and -20% in winter, and between +10% and -50% in summer. By considering the anomaly in the two future periods (Figure 3), only in the 2071-2100 period the models have a good agreement. In winter the ensemble mean anomalies are positive, between 0 and +20% (RCP2.6) and from +15 to +20% (RCP8.5); in summer the anomaly is negative, from 0 to -20% (RCP8.5).

If the model agreement in the trends is investigated (Figure 4), there is a positive trend only in winter, for RCP2.6 between +50%/100y (near future) and +100%/100y (far future); around +25%/100y for RCP8.5 (near future). The trend of precipitation appears more complex than the temperature one, due to the large uncertainty among different RCPs and models. The geographical distribution could be a further reason, as seen in the next.

The geographical distribution of the precipitation anomaly is displayed in Figure 6 for winter and summer. Unfortunately, only the far future with RCP8.5 has a good agreement among models. In winter the precipitation anomaly is positive, larger for the Alps area with respect to the flat areas (from +15 to +35% against values within +10 and +20%, respectively). In summer, the anomaly is negative, with a maximum from -15 to -25% in the pre-Alps area.

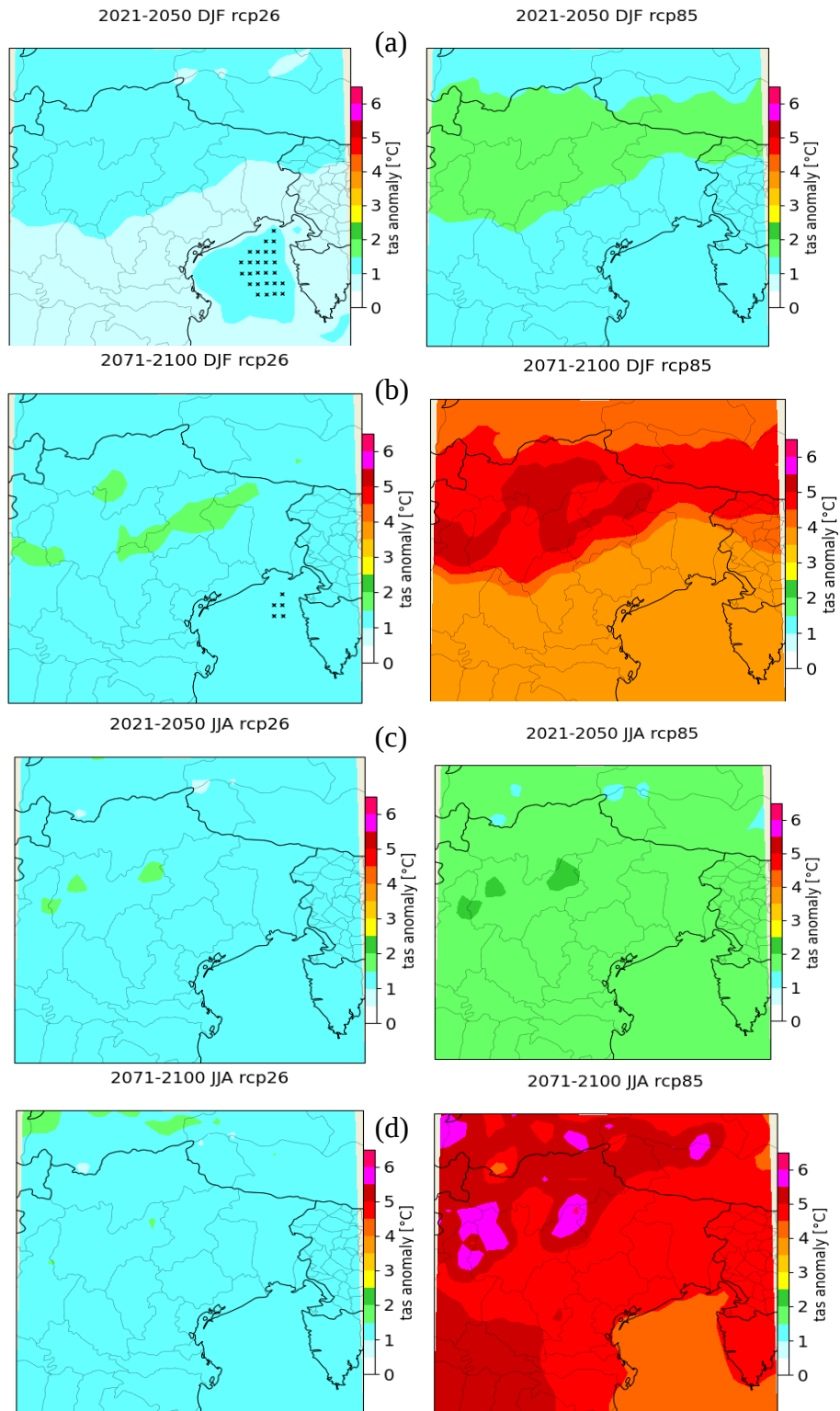


Figure 5. Geographical distribution of the temperature anomaly in winter for the 2021-2050 (rows a) and 2071-2100 (rows b) with respect to the reference period 1976-2005; the left/right hand side refer to RCP2.6/RCP8.5. Crosses indicate the grid points where the models agreement is low. Rows (c) and (d) provide the same information as (a) and (b), respectively, except they refer to summer.

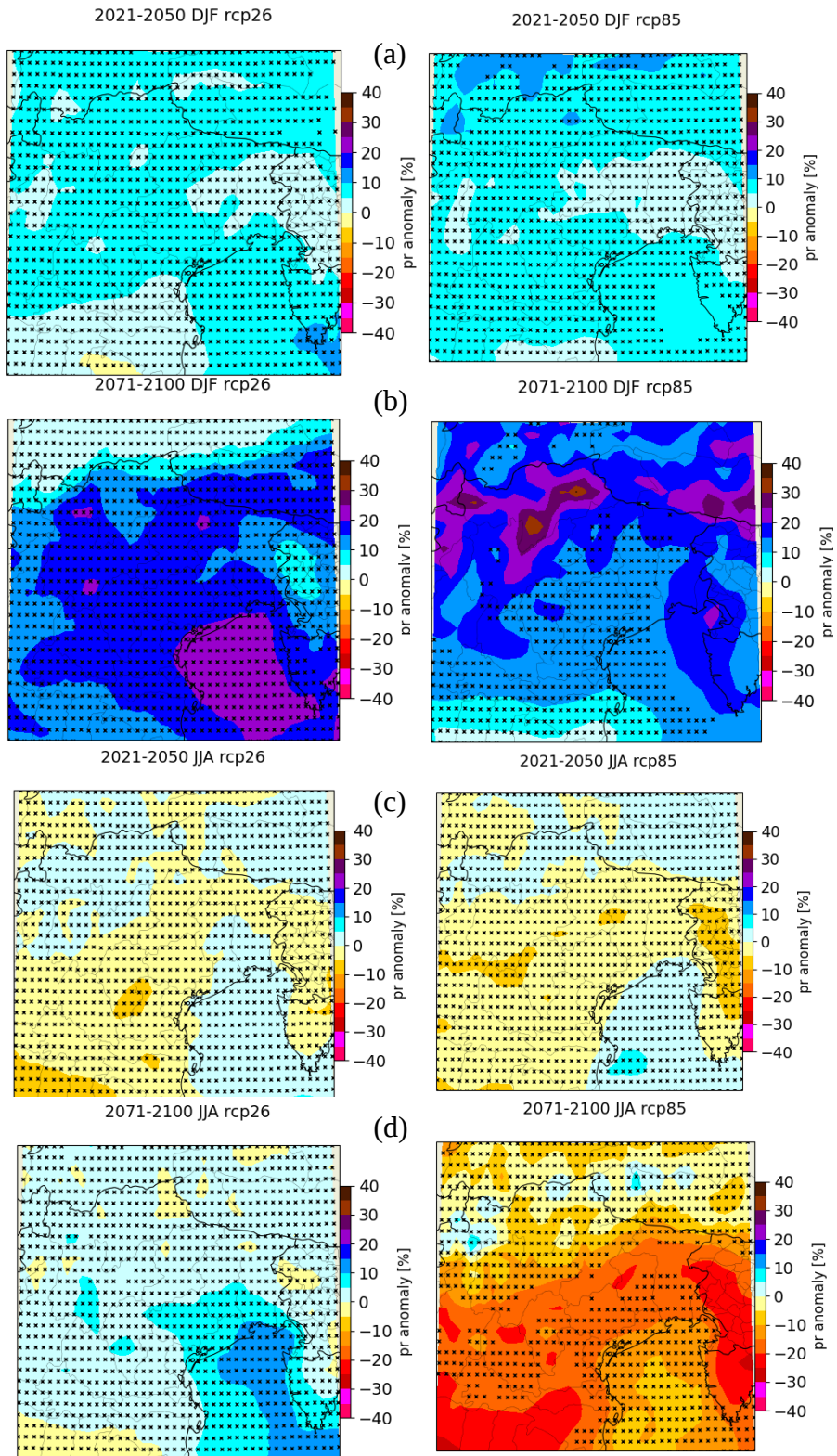


Figure 6. Geographical distribution of the precipitation anomaly (units: percent of baseline value) in winter for the 2021-2050 (row a) and 2071-2100 (row b) with respect to the reference period 1976-2005; the left/right hand side refer to RCP2.6/RCP8.5. Crosses indicate the grid points where the model agreement is low. Rows (c) and (d) provide the same information as (a) and (b), respectively, except they refer to summer.

4.3 Extreme events

In order to assess the possible changes in the frequency of extreme events and to give an idea of potential impacts, the HWDI and R95pTOT are computed for the temperature and precipitation, respectively. Figure 7 shows the geographical distribution of the number of days of heat waves anomaly (ensemble mean) for the summer for the two future periods, with respect to the reference period. In the near future, the anomaly is between 0 and 5 days, with the exception of some North Alps areas with from 5 to 10 days for RCP2.6; for RCP8.5, all the flat and mountain areas are between 5 and 10 days, whereas the coast stays within 0 and 5 days. In the far future for the RCP2.6 the anomaly are similar to the near future, but for the RCP8.5 it strongly increases: 25-30 days in coastal areas, 30-35 days in flat lands, and 35-45 days of heat waves in the Alps area.

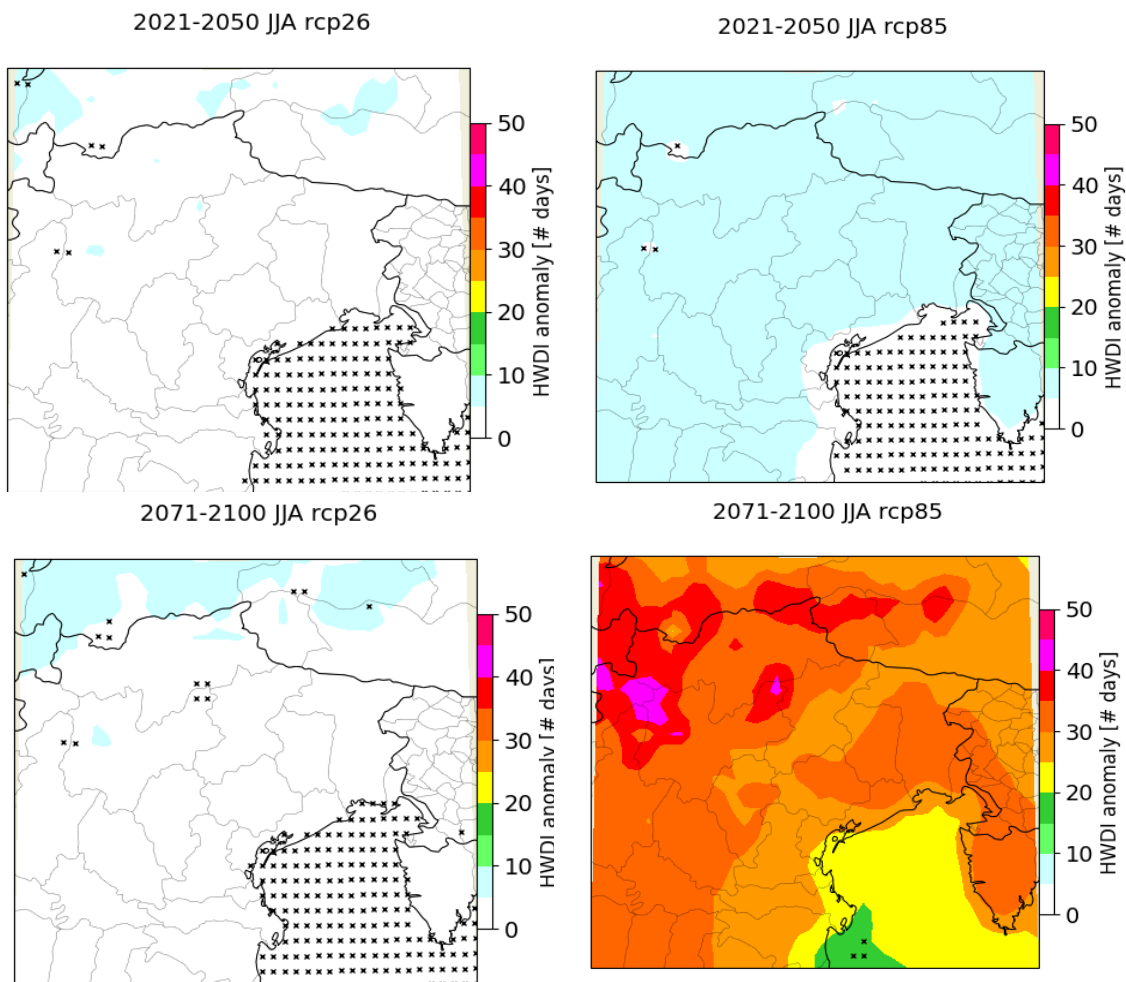


Figure 7. Geographical distribution of the heat waves duration index (HWDI) anomaly in summer for the 2021-2050 (upper panels) and 2071-2100 (lower panels) with respect to the reference period 1976-2005; the left/right hand side refer to RCP2.6/RCP8.5. Crosses indicate the grid points where the models agreement is low.

Geographical distribution of the anomaly of the cumulative precipitation larger than 95th percentile for the two forcing scenarios and future periods with respect to the reference one is shown in Figure 8 for winter and summer. Only winter with RCP8.5 has good agreement among models. In particular, in the near future there is a positive R95pTOT anomaly (from +20 to +40%) in a limited area near the Garda lake. In the far future there is an increase in the extreme precipitations in most of the domain, from +60 to +80% in the coastal areas and from +80 to +140% in the Alps areas.

5 Conclusions

This study has analyzed an ensemble of EURO-CORDEX high resolution (0.11deg) RCM simulations of the low emission RCP2.6 and high emission RCP8.5 scenarios for North-Eastern Italy for the 21st century covering. It has considered the seasonal anomalies of temperature, precipitation and annual anomalies of heat-wave duration (HWDI) and intense precipitation totals (R95pTOT). Three 30-year periods have been selected: a baseline period (from 1976 to 2005), near future (2021-2050) and far future (2071-2100).

Simulations show widespread warming in all seasons. For RCP2.6 average warming stabilizes in the range from 1°C to 1.5°C both in the near and far future and in winter and summer. For RCP8.5 warming increases from values similar to RCP2.6 in the near future to much larger values in the far future: from 3.5°C to 5°C in winter and from 4°C to 5.5°C summer. Therefore, warming is larger in summer than in winter, consistently with previous results (Zampieri et al., 2010; Coppola and Giorgi, 2010). In RCP2.6 temperature increase stops after mid 21st century, while it accelerates in RCP8.5. Warming is more spatially uniform in summer than in winter, and weaker in coastal and flat areas than in the mountain region, where it reaches 6°C in RCP8.5 and the far future against the 5°C in flat lands.

In RCP8.5 heat wave duration increases remarkably from the near to the far future especially in the mountain areas. The HWDI anomaly is 0-5 days in the coastal areas and 5-10 days in the flat and mountain areas in the near future. It grows to 25-30 days in coastal areas, 30-35 days in flat lands, and 35-45 days in the far future,.

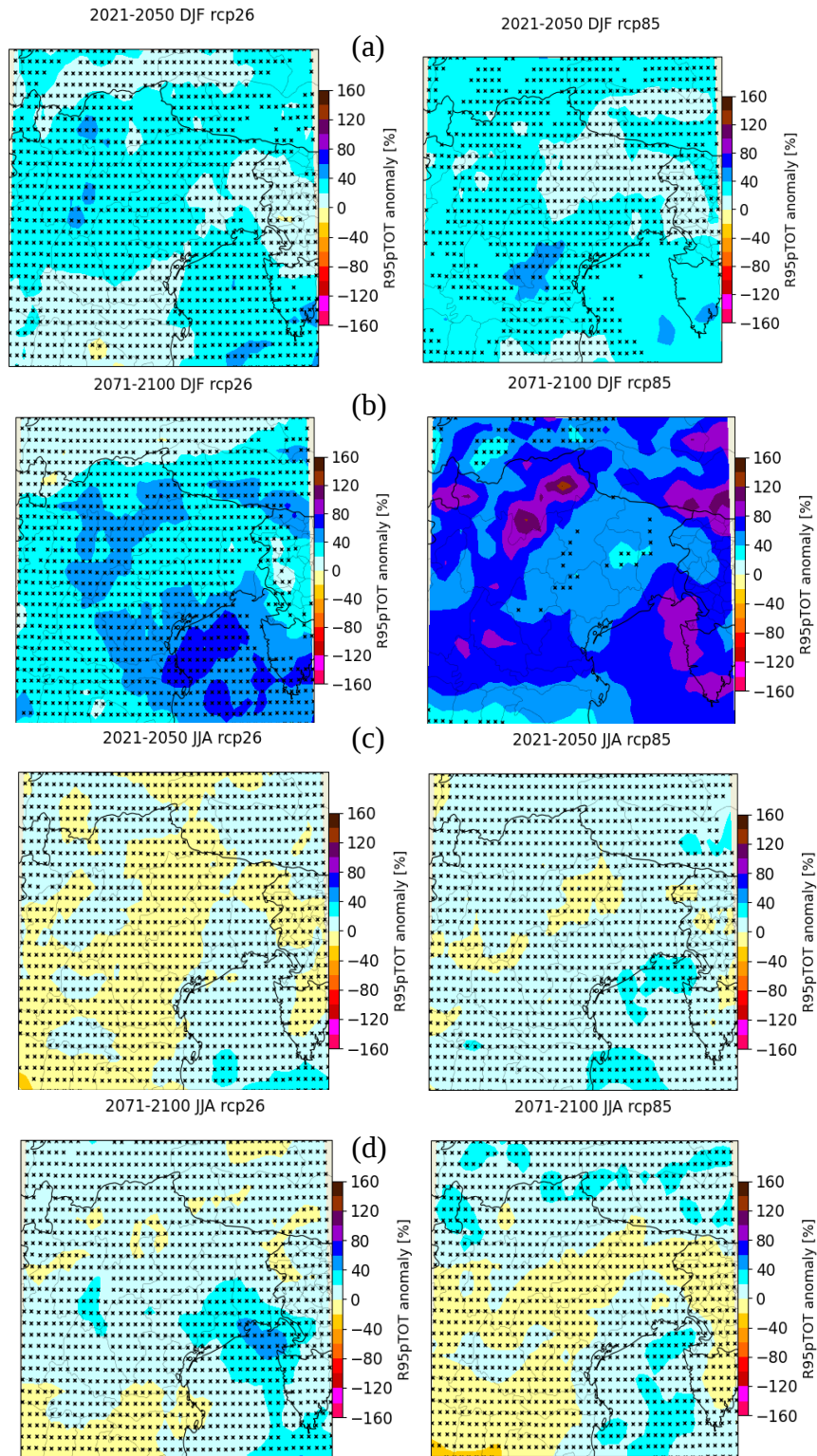


Figure 8. Geographical distribution of the cumulative precipitation larger than 95th percentile (R95pTOT) anomaly (units: percent of baseline value) in winter for the 2021-2050 (row a) and 2071-2100 (row b) with respect to the reference period 1976-2005; the left/right hand side refer to RCP2.6/RCP8.5. Crosses indicate the grid points where the model agreement is low. Rows (c) and (d) provide the same information as (a) and (b), respectively, except they refer to summer.

Climate change impact on seasonal precipitation emerges clearly only in RCP8.5, which in the far future produces a significant increase of precipitation in winter (in the range from 15% to 20%) and decrease in summer (up to -20%). RCP2.6 shows only an increase in winter in the far future, whose magnitude strongly depends on the models (from 0 to 18%), with most model suggesting a small increase (<5%). The increase of precipitation occurs mostly in the inner Alpine areas in winter, and the decrease in the flat areas and southern side of the Alps in summer (consistently with Zampieri et al., 2010; Troma et al., 2015).

The positive R95pTOT anomaly, which is present only in a limited area near the Garda lake in the RCP8.5 near future, cover most of the domain in the far future, reaching +80% in the coastal areas and +140% in the Alps.

While the positive trend of temperature shows a good agreement in the model ensemble throughout the selected region, as well as the positive and negative precipitation trend in the RCP8.5 winter and summer, respectively, the future summer precipitation for RCP2.6 is uncertain. A clear outcome of this analysis is the large differences between RCP2.6 and RCP8.5 scenarios, with a climate change signal that in the former is not everywhere and for all variable significant.

Results show the large differences between a low and a high emission scenario for climate change in North-East Italy. A high emission scenario would very likely imply large changes of mean temperature, precipitation and their extremes. This outcome stresses the importance of global mitigation actions to limit the risks caused by climate change in North-East Italy.

Acknowledgements

G. M. acknowledges ARPA FVG for providing the EURO-CORDEX regional model dataset, shortening the time to download the entire dataset, and in particular thanks Dr. Valentina Gallina for advising with CDO.

References

- Coppola, E., & Giorgi, F. (2010). An assessment of temperature and precipitation change projections over Italy from recent global and regional climate model simulations. *International Journal of Climatology: A Journal of the Royal Meteorological Society*, 30(1), 11-32.
- Cubasch, U., Meehl, G.A., Boer, G.J., Stouffer, R.J., Dix, M., Noda, A., Senior, C.A., Raper, S., Yap, K.S. (2001). Projections of future climate change, *Climate Change 2001: The Scientific Basis. Contribution of Working Group I to the Third Assessment Report of the Intergovernmental Panel on Climate Change*. Cambridge University Press, ISBN: 0521 01495 6.
- EU-CORDEX, (2017) - EURO-CORDEX Coordinated Downscaling Experiment - European Domain <http://www.euro-cordex.net/>
- Gao, X., Pal, J. S., & Giorgi, F. (2006). Projected changes in mean and extreme precipitation over the Mediterranean region from a high resolution double nested RCM simulation. *Geophysical Research Letters*, 33(3).
- Gallina, V., and Giorgi, F. 2008. Studio conoscitivo dei cambiamenti climatici e di alcuni loro impatti in Friuli Venezia Giulia, ARPA FVG .
- Giorgi, F., Mearns, L.O., 1999. Introduction to special section: regional climate modeling revisited. *Journal of Geophysical Research* 104, 6335–6352.
- Giorgi, F. (2005). Climate change prediction. *Climatic Change*, 73(3), 239-265.
- Giorgi, F. (2006). Climate change hot-spots. *Geophysical research letters*, 33(8).
- Giorgi, F., and Lionello, P. (2008). Climate change projections for the Mediterranean region. *Global and planetary change*, 63(2-3), 90-104.
- Giorgi, F., Coppola, E., Raffaele, F., Diro, G. T., Fuentes-Franco, R., Giuliani, G., ... and Torma, C. (2014). Changes in extremes and hydroclimatic regimes in the CREMA ensemble projections. *Climatic change*, 125(1), 39-51.
- IPCC (2013). *Climate Change 2013: The Physical Science Basis. Contribution of Working Group I to the Fifth Assessment Report of the Intergovernmental Panel on Climate Change* [Stocker, T.F., D. Qin, G.-K. Plattner, .. and P.M. Midgley (eds.)]. Cambridge University Press, Cambridge, United Kingdom and New York, NY, USA, 1535 pp.
- IPCC (2013). Summary for Policymakers. In: *Climate Change 2013: The Physical Science Basis. Contribution of Working Group I to the Fifth Assessment Report of the Intergovernmental Panel on*

Climate Change [Stocker, T.F., D. Qin, G.-K. Plattner, M. Tignor, S.K. Allen, J. Boschung, A. Nauels, Y. Xia, V. Bex and P.M. Midgley (eds.)]. Cambridge University Press, Cambridge, United Kingdom and New York, NY, USA.

IPCC (2014). Summary for policymakers. In: Climate Change 2014: Impacts, Adaptation, and Vulnerability. Part A: Global and Sectoral Aspects. Contribution of Working Group II to the Fifth Assessment Report of the Intergovernmental Panel on Climate Change [Field, C.B., V.R. Barros, D.J. Dokken, ... and L.L. White (eds.)]. Cambridge University Press, Cambridge, United Kingdom and New York, NY, USA, pp. 1-32.

Jacob, D., Petersen, J., Eggert, B., Alias, A., Christensen, O. B., Bouwer, L. M., ... and Georgopoulou, E. (2014). EURO-CORDEX: new high-resolution climate change projections for European impact research. *Regional environmental change*, 14(2), 563-578.

Lionello P., F. Abrantes, L. Congedi, F. Dulac, M. Gacic, D. Gomis, C. Goodess, H. Hoff, H. Kutiel, J. Luterbacher, S. Planton, M. Reale, K. Schröder, M. V. Struglia, A. Toreti, M. Tsimplis, U. Ulbrich, E. Xoplaki (2012) Introduction: Mediterranean Climate: Background Information in Lionello P. (Ed.) *The Climate of the Mediterranean Region. From the Past to the Future*, Amsterdam: Elsevier (NETHERLANDS), XXXV-IXXX, ISBN:9780124160422

Lionello, P., and Scarascia, L. (2018). The relation between climate change in the Mediterranean region and global warming. *Regional Environmental Change*, 18(5), 1481-1493.

Lionello, P., and Scarascia, L. (2020). The relation of climate extremes with global warming in the Mediterranean region and its north versus south contrast. *Regional Environmental Change*, 20(1), 1-16.

Meinshausen M, Hare B, Wigley TML, Van Vuuren D, Den Elzen MGJ et al (2006). Multi-gas emissions pathways to meet climate targets. *Clim Change* 75:151–194

Moss, R. H., Edmonds, J. A., Hibbard, K. A., Manning, M. R., Rose, S. K., Van Vuuren, D. P., ... and Meehl, G. A. (2010). The next generation of scenarios for climate change research and assessment. *Nature*, 463(7282), 747-756.

Planton, S., Lionello, P., V. Artale, R. Aznar, A. Carrillo, J. Colin, L. Congedi, C. Dubois, A. Elizalde, S. Gualdi, E. Hertig, J. Jacobeit, G. Jordà, L. Li, A. Mariotti, C. Piani, P. Ruti, E. Sanchez-Gomez, G. Sannino, F. Sevault, S. Somot, M. Tsimplis (2012) The Climate of the Mediterranean Region in Future Climate Projection in Lionello P. (Ed.) *The Climate of the Mediterranean Region. From the Past to the Future*, Amsterdam: Elsevier (NETHERLANDS), 449-502

Schulzweida, Uwe. (2019). CDO User Guide (Version 1.9.8).

<http://doi.org/10.5281/zenodo.3539275>

Stocker, T.F., D. Qin, G.-K. Plattner, L.V. Alexander, S.K. Allen, ... and S.-P. Xie (2013). Technical Summary Supplementary Material. In: Climate Change 2013: The Physical Science Basis. Contribution of Working Group I to the Fifth Assessment Report of the Intergovernmental Panel on Climate Change [Stocker, T.F., D. Qin, ... and P.M. Midgley (eds.)]. Available from www.climatechange2013.org and www.ipcc.ch.

Taylor K, Stouffer RJ, Meehl GA (2012) .An overview of CMIP5 and the experiment design. Bull Am Meteorol Soc 93:485–498.

Torma, C., Giorgi, F., & Coppola, E. (2015). Added value of regional climate modeling over areas characterized by complex terrain—Precipitation over the Alps. *Journal of Geophysical Research: Atmospheres*, 120(9), 3957-3972.

Zampieri, M., Giorgi, F., Lionello, P., & Nikulin, G., 2010. Regional climate change in the Northern Adriatic. *Physics and Chemistry of the Earth, Parts A/B/C*, 40, 32-46.